Desalination and Water Treatment
www.deswater.com

doi: 10.5004/dwt.2020.26361

205 (2020) 76–90
November

Leachate nanofiltration concentrate treatment by advanced electrochemical processes to achieve zero waste discharge: modeling and optimization

Gamze Varank

Department of Environmental Engineering, Yıldız Technical University, Davutpasa Campus, Esenler, Istanbul 34220, Turkey, Tel. +90 212.3835377; Fax +90 212.3835358; emails: gamzevarank@gmail.com/gvarank@yildiz.edu.tr (G. Varank)

Received 28 June 2020; Accepted 19 July 2020

ABSTRACT

The aim of this work is to achieve zero waste discharge in leachate treatment. Advanced electrochemical processes were applied to leachate nanofiltration concentrate formed at the nanofiltration unit of Kömürcüoda Leachate Treatment Plant. The performance of the electrochemical processes with peroxymonosulfate, peroxydisulfate and hydrogen peroxide addition as oxidants was investigated in the removal of the UV_{254} parameter–representing recalcitrant organic matter-from the leachate nanofiltration (NF) concentrate. To design and optimize the process parameters affecting the performance of electro-peroxymonosulfate (EPM), electro-peroxydisulfate (EPD) and electro-Fenton (EF) processes, central composite design (CCD) and response surface methodology (RSM) were applied. Oxidant/chemical oxygen demand ratio, current, pH, and reaction time were selected as independent variables, and the UV_{254} parameter which is at high concentrations in NF concentrate of leachate was selected as the system's response. By the application of CCD, the regression quadratic model was developed, and the data obtained were analyzed by analysis of variance. Under optimum conditions, the removal efficiencies of the UV_{254} parameter through EPM, EPD and EF processes were determined as 84.9%, 98.6% and 92.2%, respectively and the operational cost of was found to be 2.2, 3.8 and 4.7 €/m^3 for EPM, EPD and EF processes, respectively All three processes are effective advanced treatment methods for UV_{254} parameter removal from leachate NF concentrate and RSM is appropriate for designing and optimizing all three processes.

Keywords: Central composite design; Electro-Fenton; Electro-peroxydisulfate; Electro-peroxymonosulfate; Leachate nanofiltration concentrate; UV_{254} parameter

1. Introduction

One of the most important environmental issues faced in leachate treatment plants, using membrane technologies (microfiltration, ultrafiltration, nanofiltration and reverse osmosis) following biological treatment to reach high-quality effluent is the production of high volumes of membrane concentrate. Membrane concentrates contain high amounts of resistant contaminants and salt compounds [1]. The dominant constituents of dissolved organic matter in the concentrated leachate are hydrophilic organic matters and humic substances with low biodegradability [2,3]. Humic substances may be classified under three main groups consisting of humin (not soluble at all pH values), humic acid (soluble under alkali conditions) and fulvic acid (soluble in aqueous medium) [4]. He et al. [1] and Calabrò et al. [5] concluded that about 61.7%–75.0% of concentrate consists of humic acid and fulvic acid. Various treatment methods are being applied in the treatment of leachate membrane concentrates [5–11]. Recycling to the landfill, or to the membrane bioreactor is the simplest method frequently being applied but high salt concentration and humic substances in the content of concentrate inhibit the activities of

the microorganisms in the biological processes occurring in the landfill or membrane bioreactor [5,12–14]. Moreover, high concentrations of recalcitrant organic matter and salt compounds in the content of leachate's membrane concentrate cause low biodegradability. Physicochemical treatment methods are generally the first choice for membrane concentrate treatment because physicochemical methods are not only simple, low cost and effective methods in the treatment of membrane concentrate but also they are effective in the removal of recalcitrant organic matter and increasing the biodegradability [15–19]. Advanced oxidation processes are oxidation methods based on the radical generation of in principle that is being used to remove the contaminants present in water and wastewater. In the application of advanced oxidation processes for wastewater treatment hydroxyl and sulfate, radicals destroy the contaminants existing in the wastewater and offer final solutions by the transformation of the contaminants to less toxic or non-toxic forms [20].

Hydroxyl radical ($OH^{\bullet}$) is the most reactive oxidant having an oxidation potential varying in between 2.8 V (pH 0) and 1.95 V (pH 14) in water and wastewater treatment. $OH^{\bullet}$ is a nonselective oxidant readily reacting with many contaminant types. In the reaction of $OH^{\bullet}$ radicals with organic matter, carbon-centered radicals ($R^{\bullet}$ or $R^{\bullet}$–OH) form. These carbon-centered radicals then transform into organic peroxyl radicals ($ROO^{\bullet}$) in the presence of oxygen. All the radicals then react with more reactive species such as hydrogen peroxide (H_2O_2) and superoxide ($O_2^{\bullet-}$) and ensure the chemical decomposition and mineralization of organic compounds. As the half-life of hydroxyl radicals is very short, they only can be generated onsite from oxidizing agents such as H_2O_2, O_3 by the assistance of different methods such as UV, ultrasound or catalysts [20]. Photochemical and non-photochemical methods are used for hydroxyl radical generation [21].

The most widely used photochemical methods generating $OH^{\bullet}$ radical are Fenton based processes. In the Fenton process, strong reactive species form as the result of the reaction of H_2O_2 with Fe, the most commonly used transition metal for activating H_2O_2 [22]. As the Fenton reaction is effective only under acidic conditions, its application area is limited. Additionally, high amounts of iron sludge form bringing with additional costs and operational difficulty for disposal of the sludge. According to the classic Fenton treatment scheme, there are three modified Fenton processes including Fenton-like system, photo-Fenton, and electro-Fenton (EF) processes.

e-Fenton process is based on the principle of concurrent generation of H_2O_2 vs. Fe^{2+} through the reduction of molecular oxygen and iron ions, and it covers the advantages individually being provided by the electrochemical and Fenton processes. In the e-Fenton process, the higher formation of hydroxyl radicals is observed, and the oxidation strength of peroxide is higher as compared with the Fenton process [23]. The formation of hydroxyl radicals on the surface of the anode is observed as the result of oxidation of water and for higher hydroxyl radical formation hydrogen peroxide was also can be added externally. The hydroxyl radicals quickly react with compounds mostly organic in nature and as a result of this reaction the transformation of organic matter to CO_2 and H_2O, and mineralization occurs.

Peroxymonosulfate or peroxydisulfate are commonly used oxidants in sulfate radical based advanced treatment processes [24–28]. Persulfate is a strong oxidant having an oxidation potential of 2.01 V. Sulfate radicals ($SO_4^{\bullet}$) are able to be generated as the result of the activation of peroxymonosulfate or peroxydisulfate with transition metals (cobalt, Co^{2+}; iron(II), Fe^{2+}, etc), high temperature and alkali conditions or as the result of the photolysis of persulfate with high quantum yield [29–32]. As persulfate is activated, the oxidation potential of strong sulfate radicals – initiating the advanced oxidation processes – reaches the value of 2.6 V [20]. In order to obtain sulfate radicals, iron – which is cost-efficient, and nontoxic – is commonly used as a transition metal. But the slowness of regeneration following the conversion of Fe^{2+} ion to Fe^{3+} is the disadvantage of this process [33]. This problem was solved by the cathodic reduction of Fe^{3+} ions in the electro-regeneration process.

The half-life of sulfate radical is longer as compared to hydroxyl radical because hydroxyl radical is contributing to electron transfer reactions at the same time with the hydrogen – atom breakaway reaction, while the sulfate radical is only contributing to electron transfer reactions [34,35]. Hydroxyl radicals may also be generated from sulfate radicals. More hydroxyl radicals may be generated from sulfate radicals under alkali conditions [20].

Optimization is the determination of the interaction of independent variables affecting the process and of the effects of these independent variables on the response (removal efficiency) in wastewater treatment). In classic optimization models, while the effect on the system's performance of each parameter affecting the process is being examined, the experimental studies are conducted by keeping all the other parameters constant under specific conditions. In classic optimization techniques, it is not possible to reach the real optimum because the effect of interaction among the factors cannot be determined. Recently, statistical experimental design models are being applied in order to optimize the operational parameters in multi-variable systems and to obtain statistically significant models by performing a minimum number of experiments [23]. Response surface methodology (RSM) is one of the statistical techniques used for attaining maximum efficiency by optimizing the conditions in multi-variable systems. And central composite design (CCD) is one of the most commonly applied designs of RSM, which is an effective and flexible method providing sufficient data for determining the experimental error rate and effects of variables by a minimum number of experimental studies [23,36].

In the leachate treatment plant, ultrafiltration and nanofiltration membrane processes are applied to biologically treated leachate. Nanofiltration effluent meets the discharge limits suggested in the "Water Pollution Control Regulation of Turkey" but leachate nanofiltration concentrate with high recalcitrant organic matter content is disposed of the landfill. This study offers treatment alternatives for leachate concentrate by optimization of the parameters effecting the processes. The performance of electrochemical systems as EF, electro-peroxymonosulfate (EPM) and electro-peroxydisulfate (EPD) processes in the removal of UV_{254} parameter, representing recalcitrant organic matter from leachate nanofiltration concentrate was investigated. By providing leachate

nanofiltration concentrate treatment, the achievement of zero waste discharge was aimed primarily. The effects of operating parameters on the system's responses and interaction with each other were assessed by using RSM and CCD. Additionally, cost analysis of processes under optimum conditions determined by the model was determined, and the processes were compared to each other by means of removal efficiencies and cost analysis.

2. Material and methods

2.1. Leachate nanofiltration concentrate sampling and characterization

Leachate concentrate samples were obtained from the outlet of the nanofiltration unit of the leachate treatment plant of Istanbul Kömürcüoda Sanitary Landfill (41°8′ 41″N, 29°22′21″E). The leachates, arising as the result of municipal solid waste disposal at Kömürcüoda Sanitary Landfill, are treated by membrane bioreactor nanofiltration (MBR + NF) technology at the leachate treatment plant. Biologically treated leachate having an initial chemical oxygen demand (COD) value about 20,000 mg/L was exposed to sequential ultrafiltration and nanofiltration membrane processes following nitrification and denitrification processes. The concentration of effluent reaches the discharge criteria of the "Water Pollution Control Regulation of Turkey" being discharged without posing a hazard to the environment and aqueous media. And the concentrate, remaining on the nanofiltration membrane system, is recycled to the landfill. Kömürcüoda Leachate Treatment Plant had been designed to treat 1,700 m^3/d leachates. The general flow chart of the treatment plant is presented in Fig. 1.

Nanofiltration concentrate samples, obtained for experimental studies, were stored at +4°C in the laboratory in order to prevent biological and chemical reactions. Average COD, UV_{254}, total suspended solids concentrations were determined as 5,250; 3,859 and 122.5 mg/L. The pH of the concentrate was in the neutral values with the average value of 7.95. Since chloride concentration was high with the average value of 7,285 mg/L, no electrolyte addition was required for conductivity.

2.2. Experimental study and analytical procedure

The experimental studies were performed in a laboratory-scale plexiglass reactor (with a diameter of 13 cm, and height of 13 cm) having a 4 monopolar electrode set consisting of two anode and two cathode electrodes placed in parallel for the EPM, EPD and EF processes. The electrodes (6 cm width × 12 cm height, and 0.1 cm thickness), consisting of four iron plates, were placed at a distance of 1.5 cm from each other. The electrolytic solution wasn't required due to the high chloride concentration of NF concentrate samples. 500 mL sample was used for each experimental set, and the impurities on the surfaces of iron electrodes were removed with the method provided by Gengec et al. [37].

The ranges of operational parameters of the processes were determined by the use of the CCD matrix as the result of preliminary studies. In EPM, EPD and EF processes, the pH of the solution was adjusted prior to experimental studies, and a magnetic stirrer (200 rpm) was used for stirring the solution. The determined amount of oxidant was added in the wastewater sample in the electrolytic reactor prior to being exposed to electric current. All the chemicals used were of analytical-reagent grade. H_2SO_4 and NaOH solutions were used in pH adjustment. At the end of each run, the clarified effluent sample was pipetted out from the reactor after withdrawing the floated and precipitated materials. Prior to analysis, all the samples were filtered from a filter having a mesh diameter of 0.45 μm. Analysis of the characterization of the NF concentrate was conducted according to the standard methods recommended by APHA [38]. For UV_{254} parameter measurement, all samples were diluted prior to measurement and the absorbance values were measured at 254 nm by WTW 6600 UV-VIS Photolab Spectrophotometer. All measurements were carried out at 25°C. Each result was an average of three readings.

2.3. Response surface methodology and experimental design

RSM is a powerful method being used to optimize the performance of complex systems [39–41]. In RSM, mathematical and statistical techniques are used together in order to determine whether there exists a significant relationship

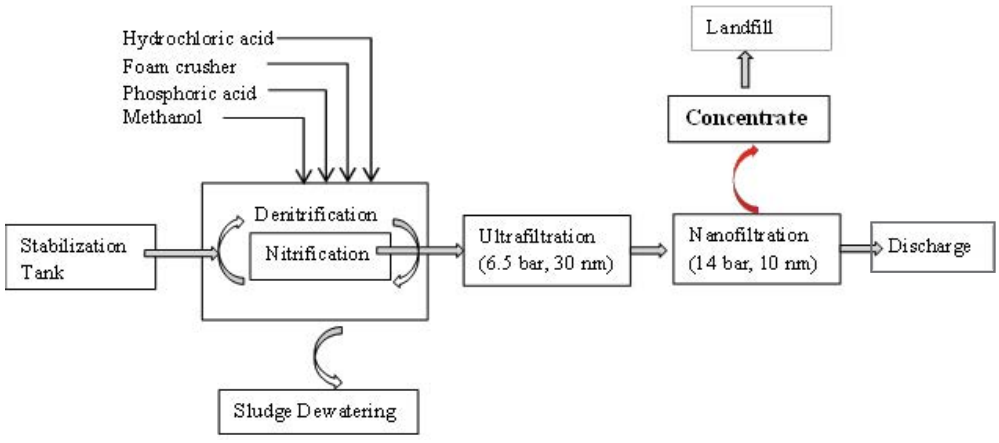

Fig. 1. General flow chart of treatment plant.

among the variables indicated as X_1, X_2, …, X_k, to determine the optimum conditions of variables affecting the system's performance, and to predict the values of the system's responses under optimum conditions [42]. By performing a preliminary experimental study, the limit values of the factors affecting the process are determined, and the experimental study is carried out under the experimental conditions defined by the model. RSM method first determines whether there exists an interaction among the variables affecting the process, and if exists, it determines which interaction is more dominant, and to which independent variable the process is more sensitive. If the system's responses are able to be described as a linear function of the independent variable, then a first-degree polynomial equation is used but if there is a curvature on the system's response surface, then the second-degree polynomial equation is used. First-degree polynomial models are inadequate for the determination of the curvature on the response surface. Generally, quadratic models are used to estimate the optimum conditions.

If the response is can be modeled by the linear function of independent variables, the approximation function is a first-degree model (Eq. (1)):

$$Y = \beta_0 + \beta_1 X_1 + \beta_2 X_2 + \varepsilon \quad (1)$$

If there is a curvature in the system, a higher polynomial degree such as second-degree model should be used (Eq. (2)):

$$Y = \beta_0 + \sum_{i=1}^{n} \beta_i X_i + \sum_{i=1}^{n} \beta_{ii} X_i^2 + \sum_{i \neq J=1}^{n} \beta_{ij} X_i X_{ij} + \varepsilon \quad (2)$$

In Eq. (2), Y refers to response value; β_0 refers to constant response value at design center point; β_i, β_{ii} and β_{ij} refer to linear, quadratic (second degree) and interactive effect regression terms respectively; X_i, refers to the level of independent variable; n refers to the number of independent variables; ε refers to random error [36].

Generally, a second-degree polynomial equation is being derived as follows:

$$Y = \beta_0 + \beta_1 X_1 + \beta_2 X_2 + \beta_3 X_3 + \beta_{12} X_1 X_2 + \beta_{13} X_1 X_3 + \beta_{23} X_2 X_3 + \beta_{11} X_1^2 + \beta_{22} X_2^2 + \beta_{33} X_3^2 + \varepsilon \quad (3)$$

While the first-degree model is defining a flat surface, the second-degree model defines a curved surface also covering the quadratic terms and interactive terms in addition to all the terms in the first-degree model. The second-degree model is also called a quadratic model. Independent variables are generally referred to as predictor variables or regressors, and thus, first degree or second-degree models are being defined as regression models.

For conformity to RSM, statistical principles, regression model techniques and optimization methods are required, and these may only be performed by the computer software [43]. In order to determine the interaction between process variables and responses, the data obtained is analyzed by analysis of variance (ANOVA). The main indicators, used to prove the model's significance and adequacy, are model *F*-value (Fisher variation ratio), probability value (Prob. *F*), and adequate precision [44]. While *F*-test is being used in order to check the statistical significance of the fit polynomial model, the model's terms are being estimated depending on the probability value (*p*-value) at a confidence level of 95% [45].

In this study, CCD – which is one of the most commonly used methods of RSM-was used for the optimization of UV_{254} parameter removal by EPM, EPD and EF processes from leachate's NF concentrate. CCD is a design tool by which the conformity is being tested after carrying out sequential experiments and obtaining sufficient data. Within the scope of the study, four factorial CCD at five levels in which 5 iterations were made at the central point, and where the total experiment set consists of 30 experiments, was applied for response surface modeling. Independent variables are oxidant/COD ratio, current, pH and reaction time for all the processes, and the system's response (dependent variable) is UV_{254} parameter removal. Coded and actual values of process' variables were determined as the result of preliminary studies and given in Table 1.

3. Results and discussion

3.1. Model developing, regression analysis, and optimization

The second-degree (quadratic) polynomial response surface model was applied to the experimental results obtained by CCD. Mathematical equations, assessing response Y (removal of UV_{254} parameter) as the function of the process independent variables (oxidant/COD ratio (*A*), current (*B*), pH (*C*), and reaction time (*D*)) were developed based on the experimental results. The UV_{254} parameter removal efficiencies (Y) being the system's response were calculated by summing up the values of constant-coefficient, four first degree effect (*A*, *B*, *C*, *D*), six interaction effect (*AB*, *AC*, *AD*, *BC*, *BD*, *CD*), and four-second degree effect (A^2, B^2, C^2, D^2) by Eqs. (4)–(6). Based on the results of the experimental design, the regression equations along with coded variables obtained by the Design Expert 11.0.1.0 software program for UV_{254} parameter removal through EPM, EPD and EF processes are given in Eqs. (4)–(6).

$$UV_{254}\text{ removal by EPM process (\%)} = 80.19 + 2.20A + 3.18B - 3.97C + 4.61D + 6.81AB + 9.44AC + 2.04AD - 7.22BC - 0.75BD - 0.14CD - 1.43A^2 - 3.45B^2 - 3.52C^2 - 3.28D^2 \quad (4)$$

$$UV_{254}\text{ removal by EPD process (\%)} = 92.65 + 4.58A + 5.29B - 4.15C + 3.34D + 1.11AB + 1.31AC + 0.16AD + 1.70BC - 0.55BD + 0.36CD - 1.09A^2 - 0.93B^2 - 3.27C^2 - 5.25D^2 \quad (5)$$

$$UV_{254}\text{ removal by EF process (\%)} = 85.23 + 3.62A + 4.17B - 1.79C + 4.45D - 0.33AB + 0.3525AC + 0.2288AD + 0.62BC + 0.03BD - 0.16CD - 1.24A^2 - 1.50B^2 + 0.70C^2 - 1.31D^2 \quad (6)$$

One factor with its coefficient indicates the partial factor effect, two factors with their coefficients indicate the interaction between two factors, and second-degree terms with their coefficients indicate the quadratic effect. In here, *A* represents oxidant/COD ratio, *B* represents the applied current, *C* represents the pH value, and *D* represents the reaction

Table 1
Coded and actual values of variables of the design of experiments for overall EPM, EPD and EF optimization

	Symbol	Factor	Coded variables				
			–2	–1	0	1	2
EPM	*A*	Oxidant/COD ratio	0.5	1	1.5	2	2.5
	B	Current (A)	0.25	1	1.75	2.5	3.25
	C	pH	3	4	5	6	7
	D	Reaction time (min)	5	15	25	35	45
EPD	*A*	Oxidant/COD ratio	0.5	1	1.5	2	2.5
	B	Current (A)	0.25	1	1.75	2.5	3.25
	C	pH	3	4	5	6	7
	D	Reaction time (min)	5	15	25	35	45
EF	*A*	Oxidant/COD ratio	0.4	0.8	1.2	1.6	2
	B	Current (A)	0.5	1.25	2	2.75	3.5
	C	pH	2	2.5	3	3.5	4
	D	Reaction time (min)	5	15	25	35	45

time, and it is being observed from Table 2 that all linear variables except pH value have a positive effect on EPM, EPD and EF processes efficiency. As the values of parameters having a positive effect increase, the removal efficiency of the UV_{254} parameter is increasing, and as the values of parameters having a negative effect increase, the removal efficiency of the UV_{254} parameter is decreasing. Among the quadratic parameters, only C^2 has a positive effect on the EF process, and all other quadratic parameters have a negative effect on EPM, EPD and EF processes. Linear means as the level of the parameter increases, the value of the response will increase but quadratic means as the level of the parameter increases the value of the response will increase until a certain level and after that, the level of the parameter will have a negative effect. This is why the linear parameter of pH has a negative effect on the EF process whereas the quadratic parameter of pH has a positive effect on the EF process. The positive marks before the terms are being expressed as a synergic effect, and negative marks are being expressed as an antagonistic effect [46]. Among the interactive parameters, *BC*, *BD*, *CD* are the ones having a negative effect on the EPM process, *BD* is the one having a negative effect on the EPD process, and *AB* and *CD* are the ones having a negative effect on the EF process. The removal efficiencies estimated by the equations and the experimental results obtained under the conditions determined by the model are compared with each other, and relevant graphs are given in Fig. 2. The high degrees of R^2 of the lines (Fig. 2) indicate that the conformity between actual and predicted values is good.

The model's statistical assessment was actualized by ANOVA, and the results of the model's ANOVA are given in Table 2. The model's probability values (*p*-values) being lower than 0.05, and the model's lack of fit (*F*-values) being higher than 0.05 indicate that the model is statistically reasonable (Table 2). *F*-values of all three processes are high, Prob. > *F*″ values are lower than 0.05 and lack of fit values is higher than 0.05. In addition, the sum of squares should definitely be considered while making an assessment regarding the reasonability of the model. The significance of the variables is also increasing along with the increase of the value of the sum of squares [46–48]. In cases where Prob. > *F*″ values are lower than 0.05, the model's terms can be expressed as significant, and in cases where Prob. > *F*″ values are lower than 0.0001, the model's terms are expressed as statistically highly significant.

As tests for specially diagnosing the competence of the model, the model's performance is provided by lack-of-fit, and pure error is based on the variance in each set of replicate measurements. In lack-of-fit, *F*-value is the ratio of the mean square of lack-of-fit to mean square of pure error. *F*-value, being a statistic parameter, allows the determination of the significance level [49]. In the model, 7.84, 16.90 and 7.77 are respectively the *F*-values for EPM, EPD and EF processes, and they indicate that the models are significant, and the probability of arising of *F*-values of this extent due to noise is 0.01%. In lack-of-fit, the *F*-values of 4.16, 3.92 and 3.59 and p values 0.06, 0.07 and 0.09 for EPM, EPD and EF processes, which were respectively, indicate that lack-of-fit is not significant as compared to the pure error.

Adequate precision is the measure of predicted response's range as compared to its associated error, and it can also be referred to as the signal-to-noise ratio. Inadequate precision, the value desired is more than 4 [50,51]. In this study, the values of adequate precision were 10.00, 15.13 and 10.87 for EPM, EPD and EF processes respectively, and it implies an adequate signal. Therefore, the design space defined by CCD can be traveled by the use of the model. Fig. 2 indicates that the responses' predicted values, provided by the model, are in conformity with the experimentally observed values. The plots, scattered close to the straight line ($y = x$), show the presence of adequate conformity between the real data and predicted data obtained by the model. The coefficient of variation (CV) is expressed as the ratio of the estimate's standard error to the observed response's mean value. If the model's CV value is lower than 10% then it can be deemed as reproducible [51,52]. The experiment's high precision and reliability can also be observed by the CV values of 9.60%, 4.15% and 4.42% obtained for the EPM, EPD and EF processes, respectively. In all three models, a good reproducibility was indicated by the CV values which were less than 10%.

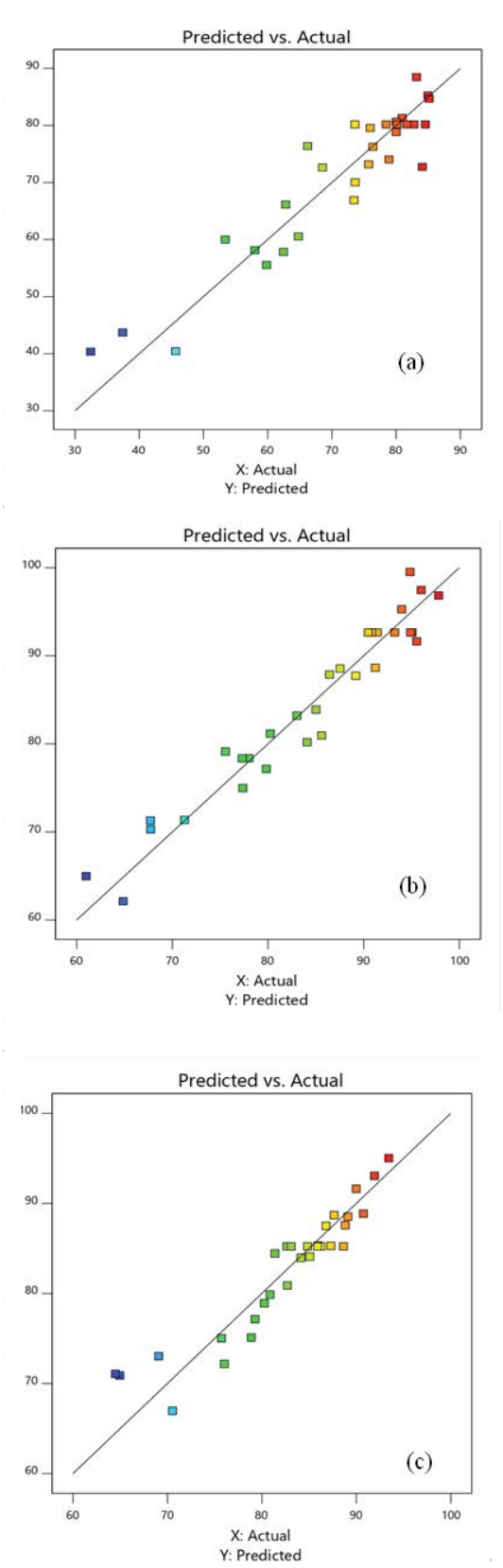

Fig. 2. Regression plots of actual data against predicted values from the response surface models describing humic matter removal by (a) EPM, (b) EPD and (c) EF processes.

The model's conformity can also be verified through the coefficient of determination which is between 0 and 1. R^2 values are 0.88, 0.94 and 0.88, and it indicates that the quadratic model can be used to explain 88%, 94% and 88% of the variability in the response. These values imply that only 12% of the total variation for the EPM process, that only 6% of the total variation for the EPD process, and that only 12% of the total variation for the EF process is not explainable by the empirical model. As the determination coefficient has a value higher than 0.80 then the state of conformity can be referenced [41]. Having the model's correlation coefficient values higher than the value 0.80 for all three processes indicates that the process is explainable by the regression models and that the response surface model applied in estimating the efficiencies of UV_{254} parameter removal in the study performed is giving results of acceptable adequacy. Adjusted R^2 can be used in order to correct the model's factor number and the sample size. But, R^2 always increases by the inclusion of a variable in the model no matter whether the included variable is statistically significant or not [53]. Thus, the use of adjusted R^2 is being preferred by some researchers. The adjusted R^2 is not subject to a gradual increase by the inclusion of variables in the model. Actually, the adjusted R^2's value is often decreasing by the inclusion of unnecessary variables in the model. We may reveal the inclusion of insignificant variables in the model through a high level of difference between R^2 and adjusted R^2 [54]. Here, an adjusted R^2 value of 0.77, 0.88 and 0.77 has been found to be relatively close to the value of R^2.

Three-dimensional plots (3D plots) of the regression models were used in order to graphically describe the interactions. Response surface plots obtained by the quadratic equations are given in Figs. 3–5. Response surface plots obtained by the use of software programs indicate the three-dimensional view of UV_{254} parameter removal in different combinations of the independent variables. If the interaction among independent variables is significant, the curvature of the three-dimensional surface is being observed clearly. If the response surface plots have distinct peak values, it means that the optimum conditions providing the maximum values of the responses depend on all of the variables [23]. Since maximum removal efficiencies are obtained at optimum conditions, removal efficiency decreases as moving away from these points so higher or lower values of the variables are not desired.

In Figs. 3 and 4, the effect of variables on the UV_{254} removal by EPM and EPD processes is given. As seen in the figure, the reaction time and current value directly affect persulfate activation, because as per the Faraday's law, Fe(II) formation increases depending on the increasing reaction time and current. Removal of organic matter actualizes over two mechanisms: Coagulation (via (Fe(OH)*n*) and oxidation (SO_4^-). The 5–9 range of pH value doesn't have any effect on the organic matter removal. This condition may be explained in two manners, Fe based coagulation mechanism is effective at the pH range of 4–9, and it is independent of pH at this range. Secondly, sulfate radicals are active under acidic conditions (pH < 7), and they form hydroxyl radicals by reacting with hydroxyl ions in the presence of hydroxyl ions (pH > 7), and hydroxyl radicals are effective strong oxidants in the decomposition of organic compounds [55–57].

Table 2
ANOVA results of the response surface model of EPM, EPD and EF processes

Source	Sum of squares	Df	Mean square	*F*-ratio	*p*-value	Remark
EPM						
Model (EPM)	5,078.59	14	362.76	7.84	0.0001	Significant
A-oxidant/COD ratio	116.16	1	116.16	2.51	0.1340	Not significant
B-current (A)	243.08	1	243.08	5.25	0.0368	Significant
C-pH	378.10	1	378.10	8.17	0.0120	Significant
D-reaction time (min)	510.05	1	510.05	11.02	0.0047	Significant
AB	741.75	1	741.75	16.03	0.0012	Significant
AC	1,426.20	1	1,426.20	30.82	<0.0001	Highly significant
AD	66.50	1	66.50	1.44	0.2492	Not Significant
BC	835.21	1	835.21	18.05	0.0007	Significant
BD	9.06	1	9.06	0.1958	0.6645	Not significant
CD	0.3364	1	0.3364	0.0073	0.9332	Not significant
A^2	56.47	1	56.47	1.22	0.2867	Not significant
B^2	326.90	1	326.90	7.06	0.0179	Significant
C^2	340.78	1	340.78	7.36	0.0160	Significant
D^2	295.73	1	295.73	6.39	0.0232	Significant
Residual	694.13	15	46.28			
Lack of fit	619.61	10	61.96	4.16	0.0646	Not significant
Pure error	74.52	5	14.90			
Cor. total	5,772.72	29				
EPD						
Model (EPD)	2,888.36	14	206.31	16.90	<0.0001	Highly significant
A-oxidant/COD ratio	504.35	1	504.35	41.31	<0.0001	Highly significant
B-current (A)	670.35	1	670.35	54.90	<0.0001	Highly significant
C-pH	412.51	1	412.51	33.79	<0.0001	Highly significant
D-reaction time (min)	268.00	1	268.00	21.95	0.0003	Significant
AB	19.62	1	19.62	1.61	0.2242	Not significant
AC	27.30	1	27.30	2.24	0.1556	Not significant
AD	0.4489	1	0.4489	0.0368	0.8505	Not significant
BC	46.31	1	46.31	3.79	0.0704	Not significant
BD	4.80	1	4.80	0.3928	0.5402	Not significant
CD	2.06	1	2.06	0.1687	0.6871	Not significant
A^2	32.40	1	32.40	2.65	0.1241	Not significant
B^2	23.50	1	23.50	1.92	0.1856	Not significant
C^2	292.51	1	292.51	23.96	0.0002	Significant
D^2	754.74	1	754.74	61.81	<0.0001	Highly significant
Residual	183.15	15	12.21			
Lack of fit	162.44	10	16.24	3.92	0.0723	Not significant
Pure error	20.71	5	4.14			
Cor. total	3,071.50	29				

(Continued)

Table 2 Continued

Source	Sum of squares	Df	Mean square	*F*-ratio	*p*-value	Remark
EF						
Model (EF)	1,450.15	14	103.58	7.77	0.0002	Significant
A-oxidant/COD ratio	314.07	1	314.07	23.56	0.0002	Significant
B-current (A)	416.50	1	416.50	31.25	<0.0001	Highly significant
C-pH	77.26	1	77.26	5.80	0.0294	Significant
D-reaction time (min)	475.26	1	475.26	35.66	<0.0001	Highly significant
AB	1.76	1	1.76	0.1317	0.7217	Not significant
AC	1.99	1	1.99	0.1492	0.7048	Not significant
AD	0.8372	1	0.8372	0.0628	0.8055	Not significant
BC	6.15	1	6.15	0.4614	0.5073	Not significant
BD	0.0132	1	0.0132	0.0010	0.9753	Not significant
CD	0.4225	1	0.4225	0.0317	0.8611	Not significant
A^2	42.02	1	42.02	3.15	0.0961	Not significant
B^2	61.53	1	61.53	4.62	0.0484	Significant
C^2	13.48	1	13.48	1.01	0.3305	Not significant
D^2	47.36	1	47.36	3.55	0.0790	Not significant
Residual	199.94	15	13.33			
Lack of fit	175.47	10	17.55	3.59	0.0857	Not significant
Pure error	24.47	5	4.89			
Cor. total	1,650.09	29				

At constant current values, as reaction time increases more iron ions are dissolved from the electrodes and iron concentration activating PS increases. The increase in PS dose increases the possibility of sulfate radical formation. As PS/COD ratio reaches high values, the number of sulfate radicals increase and the excess sulfate radicals in the solution react with each other instead of reacting with the organic matter resulting in persulfate formation again [58] (Eqs. (7)–(8)). As persulfate is a weaker oxidant compared to sulfate radicals, the removal efficiency of organic matter also decreases. Similar results were obtained by Rao et al. [59] and Jaafarzadeh et al. [60].

$$SO_4^{\bullet -} + SO_4^{\bullet -} \rightarrow S_2O_8^{-2} \quad (7)$$

$$S_2O_8^{-2} + SO_4^{\bullet -} \rightarrow S_2O_8^{\bullet -} + SO_4^{-2} \quad (8)$$

Current is one of the most significant parameters for the EF process effecting both performance of the treatment process and the cost of the energy. The optimum current value for the EF process was found to be 3.05 and it can be seen from Fig. 5 that UV_{254} removal efficiency decreases moving away from the optimum value. H_2O_2 formation is not sufficient at low current values, and due to the reactions occurring at the anode and the cathode, O_2 and H_2 accumulate and settle at high current values [61,62]. UV_{254} removal efficiency increase to specific reaction time, and then that decreases. In the EF process under strongly acidic conditions, Fe dissolving from the electrodes oxidizes to Fe^{2+} and a specific amount of H_2O_2 forms between anode and cathode resulting in hydroxyl radical formation. These oxidants oxidize the organic matter in the wastewater in a short while. And then the efficiency of removal decreases, and the reaction becomes stable gradually [61]. The optimum pH range for the EF process is between 2 and 4 [63]. H_2O_2 enabling hydroxyl radical formation is generated at low pH values. Fe^{2+} oxidizes to $Fe(OH)_2$ and then converts to $Fe(OH)_3$ over the pH values of 5 causing a significant decrease in hydroxyl radical formation. In this study, as the pH range for the EF process was selected between 2 and 4, no significant change in UV_{254} removal efficiency was observed at this pH range. UV_{254} removal rate increases as the amount of H_2O_2 increases due to oxidant dosing. After reaching a specific value removal efficiency decreases. This decrease may be explained by the excess peroxide amount resulting from the consumption of free hydroxyl radicals [64].

Graphical Pareto analysis provides significant information about the effect of the factors. The contribution value of each parameter on UV_{254} removal from leachate NF concentrate by advanced electrocoagulation processes is being calculated by the following equation:

$$P_i = \frac{b_i^2}{\sum b_i^2} \times 100\left(i \neq 0\right) \quad (9)$$

In here, b_i is the numerical coefficient effect of factor *i*. It is being observed from Fig. 6 among linear parameters that reaction time and current, among quadratic parameters current, pH and reaction time among interactive parameters oxidant/COD ratio *x*pH and current *x*pH are found to be effective in the UV_{254} removal by EPM process. In the removal of UV_{254} by the EPD process, all of the linear parameters, quadratic parameters of pH and reaction time are effective. All linear parameters and all quadratic parameters except for

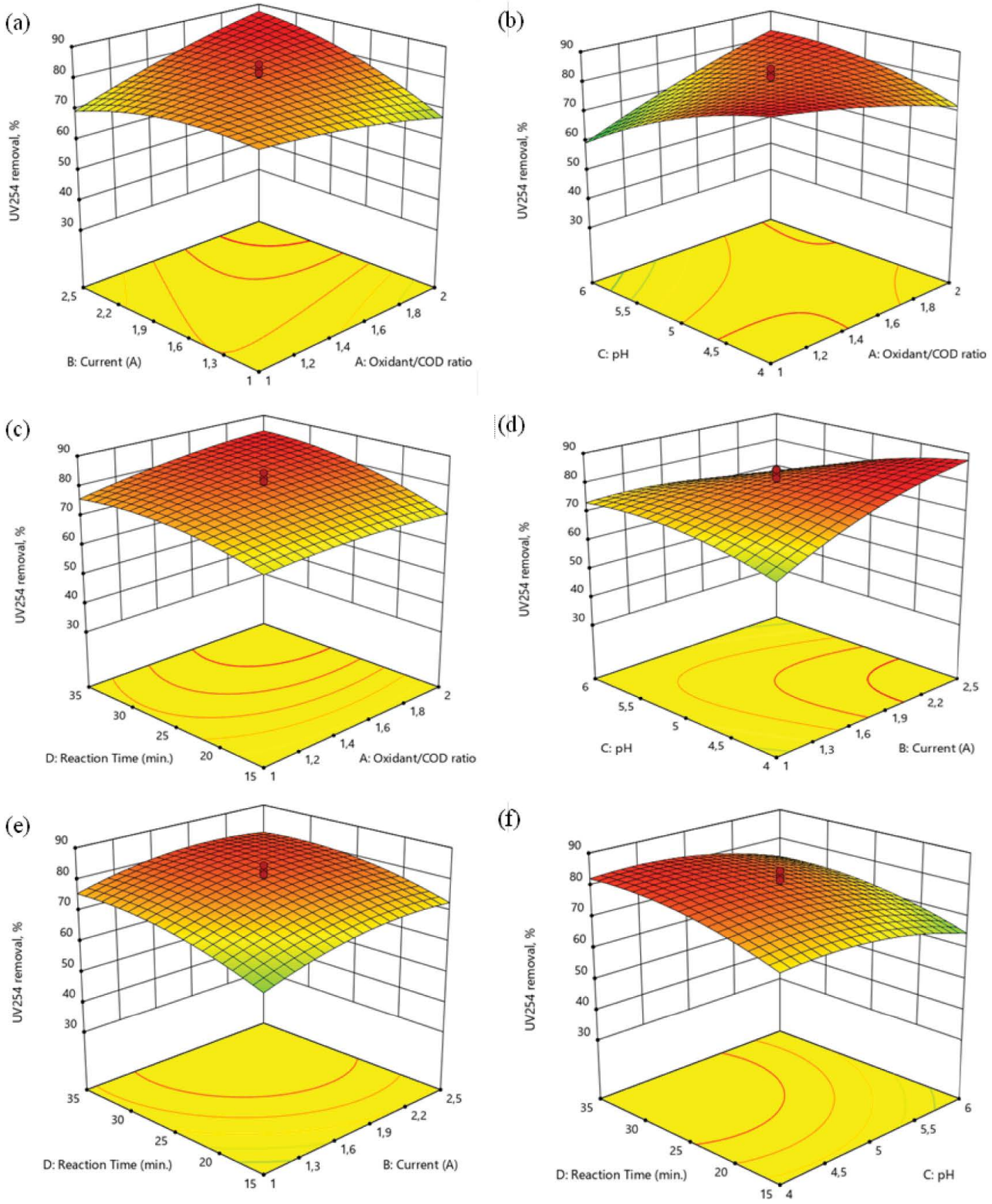

Fig. 3. The quadratic response surface plot of humic matter removal efficiency by EPM process (a) effect of oxidant/COD ratio and current, (b) effect of oxidant/COD ratio and pH, (c) effect of oxidant/COD ratio and time, (d) effect of pH and current, (e) effect of current and time and (f) effect of pH and time.

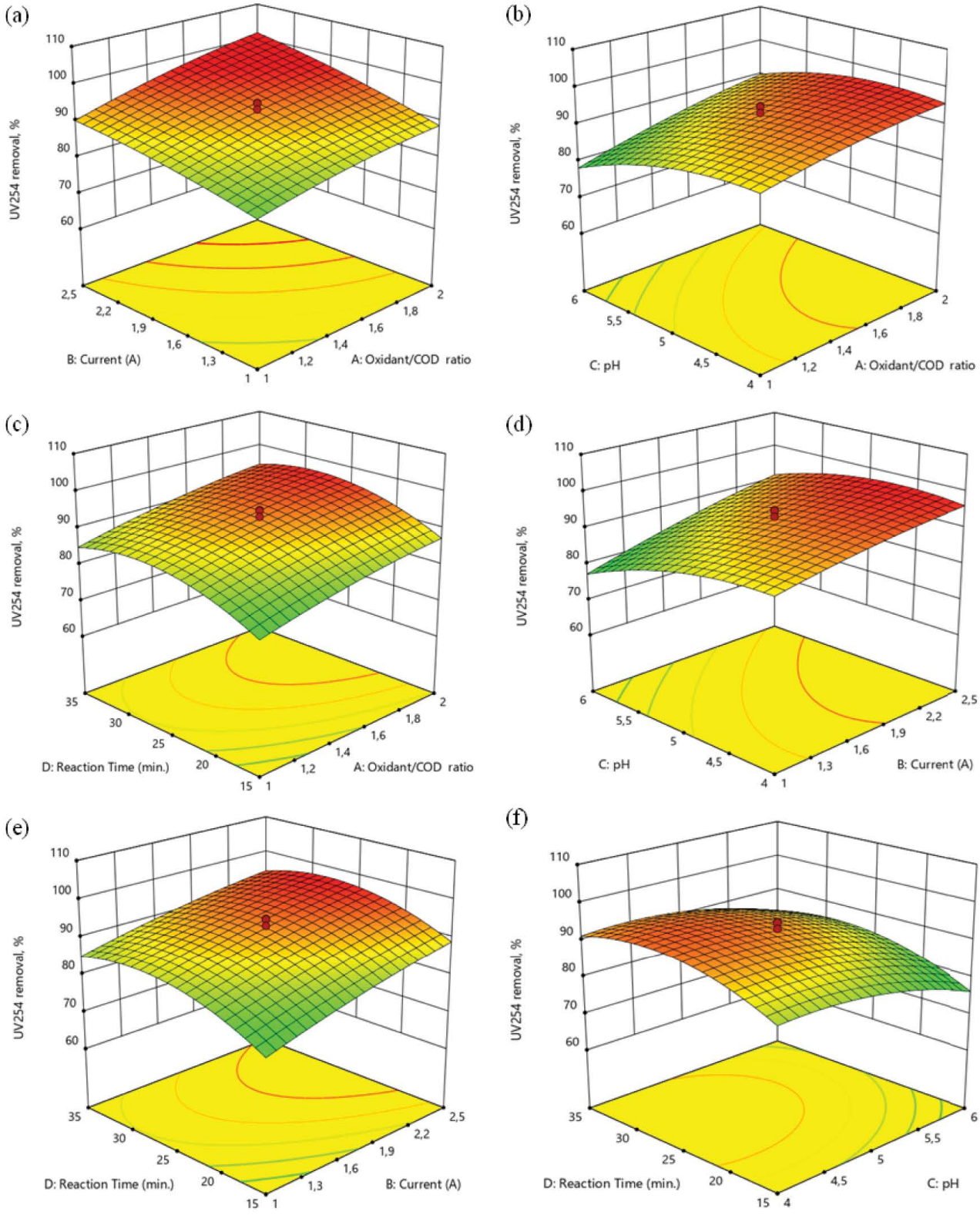

Fig. 4. The quadratic response surface plot of humic matter removal efficiency by EPD process (a) effect of oxidant/COD ratio and current, (b) effect of oxidant/COD ratio and pH, (c) effect of oxidant/COD ratio and time, (d) effect of pH and current, (e) effect of current and time and (f) effect of pH and time.

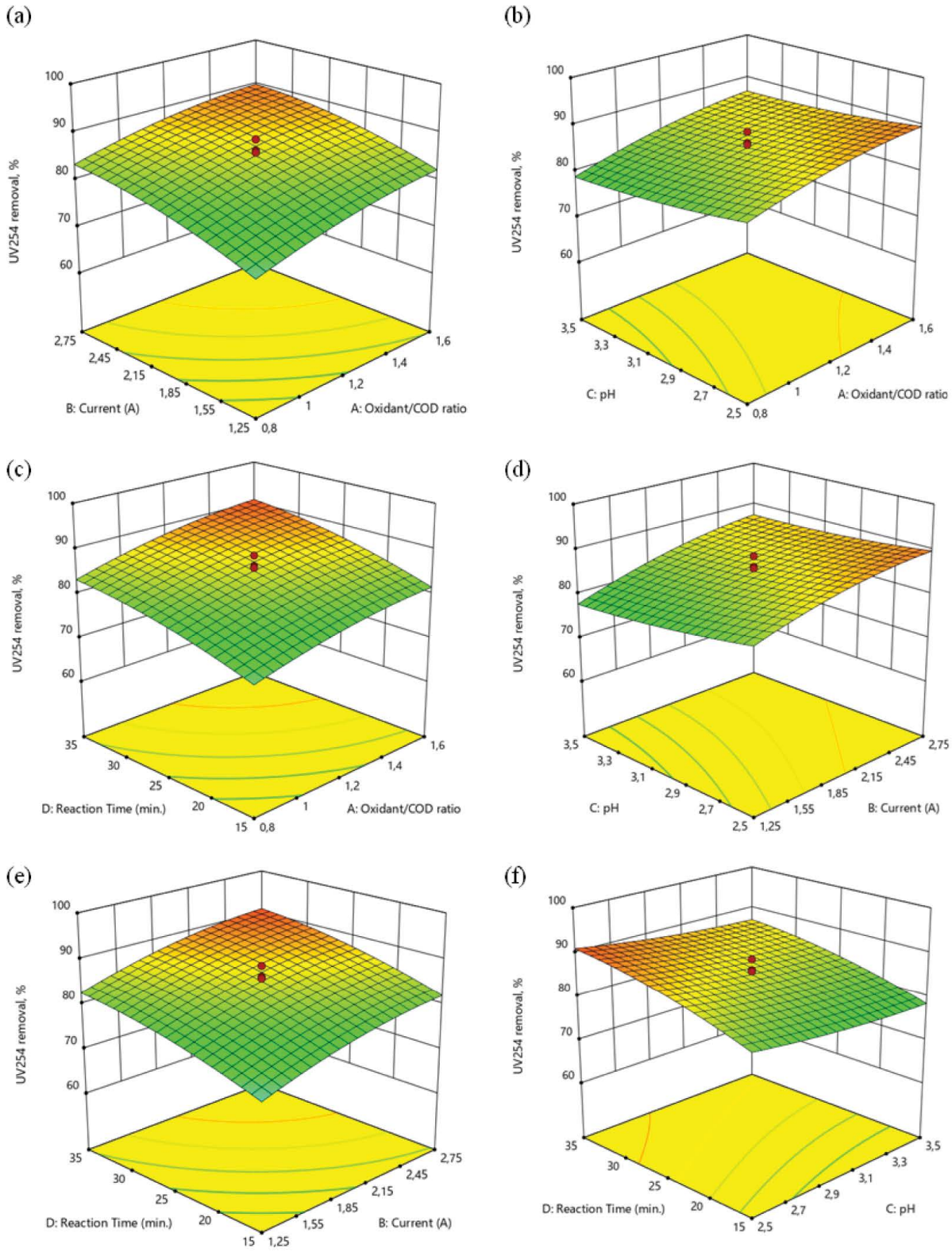

Fig. 5. The quadratic response surface plot of humic matter removal efficiency by EF process (a) effect of oxidant/COD ratio and current, (b) effect of oxidant/COD ratio and pH, (c) effect of oxidant/COD ratio and time, (d) effect of pH and current, (e) effect of current and time and (f) effect of pH and time.

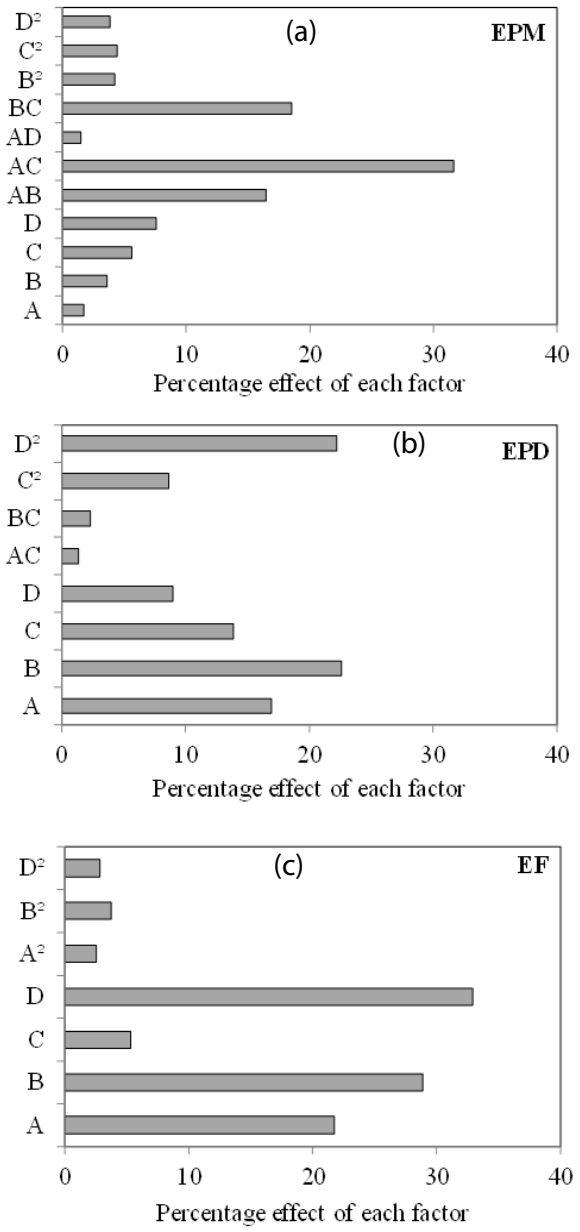

Fig. 6. Pareto curve for UV_{254} removal by (a) EPM, (b) EPD and (c) EF processes.

pH are effective on the UV_{254} parameter by EF processes. The results obtained by the Pareto analysis are in conformity with the results of ANOVA.

The numerical optimization method was used for obtaining the optimum conditions ensuring the attainment of maximum UV_{254} removal efficiency. Under optimum conditions (oxidant/COD ratio of 1.07, current of 1.85, pH value of 4.1 and reaction time of 30.5 min for EPM process; oxidant/COD ratio of 1.94, current of 2.41, pH value of 5.3 and reaction time of 32.4 min for EPD process; oxidant/COD ratio of 1.57, current of 2.17, pH value of 2.5 and reaction time of 34.0 min for EF process) UV_{254} parameter removal efficiencies predicted by the second-degree response surface model were determined as 86.34%, 99.41% and 93.56% for EPM, EPD and EF processes respectively. And the removal efficiencies obtained as the result of experimental studies under optimum conditions determined by the model are 84.9%, 98.6% and 92.2% for EPM, EPD and EF processes respectively. The experimentally obtained removal efficiencies are found to be very close to the removal efficiencies predicted by the model. The use of CCD is a successful strategy in the determination of optimum conditions for obtaining maximum removal efficiency of UV_{254} parameter removal from leachate's NF concentrate through EPM, EPD and EF processes.

In literature, there are studies regarding the treatment of leachate membrane concentrate and removal of UV_{254} parameter removal through various advanced treatment methods [65–68] but there is a deficiency in modeling and optimization of UV_{254} parameter removal from leachate membrane concentrate by electrochemical processes especially using persulfates. When the results of the present study are compared with the results of studies covering leachate membrane concentrate treatment by advanced oxidation processes in literature, it can be concluded that the removal efficiencies obtained in this study are found to be higher. Huang et al. [29] reported 81.8% UV_{254} parameter removal by combined coagulation-micro-electrolysis with hydrogen peroxide addition. Wang et al. [68] investigated leachate nanofiltration and reverse osmosis concentrate treatment by ozonation and obtained 58.13% and 39.81% UV_{254} parameter removal efficiencies for reverse osmosis and nanofiltration concentrates, respectively. Zhang et al. [67] concluded 83% UV_{254} parameter removal from leachate reverse osmosis concentrate by the microwave-Fenton process. Chen et al. [66] concluded 94.37% UV_{254} parameter removal from leachate membrane concentrate by combined coagulation ozonation process. In the present study 84.7%, 97.1% and 91.8% UV_{254} parameter removal efficiencies are determined by EPM, EPD and EF process under optimum conditions, respectively.

3.2. Operational cost

Operating cost is one of the most significant parameters used besides process efficiency in the decision of applicability of any wastewater treatment process. The operating cost is calculated by the following equation [69].

$$\text{Operational cost} = \text{ENC} + \text{ELC} + C_{\text{chemical}} \tag{10}$$

In the equation, C_{energy} value indicates the energy consumption (kWh/m^3), $C_{\text{electrode}}$ value indicates the electrode consumption (kg/m^3), and C_{chemical} value indicates the consumption of chemical added in electrolytic reactor (kg/m^3). The main operating cost component in EPM, EPD and EF processes is electrical energy consumption being expressed as C_{energy}. Electrical energy consumption is being calculated by the use of Eq. (47) [65].

$$\text{ENC} = \frac{U \times I \times t}{V} \tag{11}$$

In this equation, $C_{electrode}$ expresses the energy consumption (kWh/m^3), U expresses the applied voltage (V), I expresses the current density (A), t expresses the reaction period (h), and V expresses the treated wastewater amount (L).

The dissolved electrode amount is theoretically being calculated by the use of Faraday laws.

$$\mathrm{ELC} = \frac{I \times t \times M_w}{Z \times F \times V} \quad (12)$$

In this equation, C (g/L) expresses the iron concentration in electrolysis cell, I expresses the current density (A), t expresses the reaction time (h), M expresses the molecular weight of anode (g/mol), Z expresses the chemical equivalence, F expresses the Faraday constant (96,500 C/mol), and V expresses the volume of treated wastewater (L).

The cost of the energy of the three processes was calculated to be 0.7, 2.0 and 2.5 €/m^3 for EPM, EPD and EF processes; the cost of electrodes was calculated to be 1.0, 1.4 and 2.1 €/m^3 for EPM, EPD and EF processes and the cost of the chemicals was calculated to be 0.5, 0.4 and 0.12 €/m^3 for EPM, EPD and EF processes. Consequently, in the treatment of leachate's NF concentrate, the total cost was determined as 2.2, 3.8 and 4.7 €/m^3 for EPM, EPD and EF processes respectively. The process with the highest operating cost was determined as EF, and the process with the lowest operating cost was determined as EPM.

4. Conclusion

In this study, CCD and RSM were applied for the determination of optimal operating conditions of EPM, EPD and EF processes to obtain maximum removal efficiency of the UV_{254} parameter from leachate's NF concentrate and statistically reliable results were obtained. A high degree of conformity was determined among the quadratic models and experimental data. Variance analysis had indicated high determination coefficient values. Experimentally obtained UV_{254} removal efficiencies under optimum conditions were 84.9%, 98.6% and 92.2% for EPM, EPD and EF processes, respectively. It can be concluded that EPM, EPD and EF processes are effective processes in the removal of the UV_{254} parameter from leachate's NF concentrate and that the models developed by CCD and RSM for the three processes have statistically high significance level. With the help of the applied methodology, it had been possible to estimate the experimental results as close to accurate and to determine the quadratic and EF processes are highly efficient processes in humic substance removal from leachate's NF concentrate. Although three of the processes showed higher removal rates, based on the operating cost it can be said that, EPM process has the lowest operational cost with high removal efficiency.

References

[1] R. He, B.H. Tian, Q.Q. Zhang, H.T. Zhang, Effect of Fenton oxidation on biodegradability, biotoxicity and dissolved organic matter distribution of concentrated landfill leachate derived from a membrane process, Waste Manage., 38 (2015) 232–239.

[2] Q.-Q. Zhang, B.-H. Tian, X. Zhang, A. Ghulam, C.-R. Fang, R. He, Investigation on characteristics of leachate and concentrated leachate in three landfill leachate treatment plants, Waste Manage., 33 (2013) 2277–2286.

[3] B.O. Clarke, T. Anumol, M. Barlaz, S.A. Snyder, Investigating landfill leachate as a source of trace organic pollutants, Chemosphere, 127 (2015) 269–275.

[4] F.J. Stevenson, Humus Chemistry: Genesis, Composition, Reactions, Wiley, New York, 1994.

[5] P.S. Calabrò, S. Sbaffoni, S. Orsi, E. Gentili, C. Meoni, The landfill reinjection of concentrated leachate: findings from a monitoring study at an Italian site, J. Hazard. Mater., 181 (2010) 962–968.

[6] Y. Deng, J.D. Englehardt, Electrochemical oxidation for landfill leachate treatment, Waste Manage., 27 (2007) 380–388.

[7] S.Y. Hunce, D. Akgul, G. Demir, B. Mertoglu, Solidification/stabilization of landfill leachate concentrate using different aggregate materials, Waste Manage., 32 (2012) 1394–1400.

[8] X.Y. Li, L.W. Zhang, C.W. Wang, Review of disposal of concentrate streams from nanofiltration (NF) or reverse osmosis (RO) membrane process, Adv. Mater. Res., (2012) 3470–3475.

[9] G. Pérez, J. Saiz, R. Ibañez, A.M. Urtiaga, I. Ortiz, Assessment of the formation of inorganic oxidation by-products during the electrocatalytic treatment of ammonium from landfill leachates, Water Res., 46 (2012) 2579–2590.

[10] W.-W. Tang, G.-M. Zeng, J.-L. Gong, J. Liang, P. Xu, C. Zhang, B.-B. Huang, Impact of humic/fulvic acid on the removal of heavy metals from aqueous solutions using nanomaterials: a review, Sci. Total Environ., 468–469 (2014) 1014–1027.

[11] X. Qi, C. Zhang, Y. Zhang, Treatment of Landfill Leachate RO Concentrate by VMD, International Conference on Circuits and Systems (CAS 2015), Paris, France.

[12] I.A. Tałałaj, Release of heavy metals on selected municipal landfill during the calendar year, Rocz. Ochr. Sr., 16 (2014) 404–420.

[13] S. Chen, D. Sun, J.-S. Chung, Simultaneous removal of COD and ammonium from landfill leachate using an anaerobic-aerobic moving-bed biofilm reactor system, Waste Manage., 28 (2008) 339–346.

[14] C. Fang, K. Boe, I. Angelidaki, Anaerobic co-digestion of desugared molasses with cow manure; focusing on sodium and potassium inhibition, Bioresour. Technol., 102 (2011) 1005–1011.

[15] Y.Y. Long, J. Xu, D.S. Shen, Y. Du, H.J. Feng, Effective removal of contaminants in landfill leachate membrane concentrates by coagulation, Chemosphere, 167 (2017) 512–519.

[16] C. Amor, E. De Torres-Socías, J.A. Peres, M.I. Maldonado, I. Oller, S. Malato, M.S. Lucas, Mature landfill leachate treatment by coagulation/flocculation combined with Fenton and solar photo-Fenton processes, J. Hazard. Mater., 286 (2015) 261–268.

[17] S.K. Singh, W.Z. Tang, Statistical analysis of optimum Fenton oxidation conditions for landfill leachate treatment, Waste Manage., 33 (2013) 81–88.

[18] H.W. Wang, Y.-N. Wang, X.Y. Li, Y.J. Sun, H. Wu, D. Chen, Removal of humic substances from reverse osmosis (RO) and nanofiltration (NF) concentrated leachate using continuously ozone generation-reaction treatment equipment, Waste Manage., 56 (2016) 271–279.

[19] S.E.H. Comstock, T.H. Boyer, K.C. Graf, Treatment of nanofiltration and reverse osmosis concentrates: comparison of precipitative softening, coagulation, and anion exchange, Water Res., 45 (2011) 4855–4865.

[20] Y. Deng, R. Zhao, Advanced oxidation processes (AOPs) in wastewater treatment, Curr. Pollut. Rep., 1 (2015) 167–176.

[21] R. Munter, Advanced oxidation processes – current status and prospect, Proc. Estonian Acad. Sci. Chem., 50 (2001) 59–80.

[22] J.J. Pignatello, E. Oliveros, A. MacKay, Advanced oxidation processes for organic contaminant destruction based on the Fenton reaction and related chemistry, Crit. Rev. Env. Sci. Technol., 36 (2006) 1–84.

[23] S. Mohajeri, H.A. Aziz, M.H. Isa, M.A. Zahed, M.N. Adlan, Statistical optimization of process parameters for landfill leachate treatment using electro-Fenton technique, J. Hazard. Mater., 176 (2010) 749–758.

[24] X.X. Jiang, Y.L. Wu, P. Wang, H.J. Li, W.B. Dong, Degradation of bisphenol A in aqueous solution by persulfate activated with ferrous ion, Environ. Sci. Pollut. Res., 20 (2013) 4947–4953.
[25] Y.-H. Guan, J. Ma, Y.-M. Ren, Y.-L. Liu, J.-Y. Xiao, L.-Q. Lin, C. Zhang, Efficient degradation of atrazine by magnetic porous copper ferrite catalyzed peroxymonosulfate oxidation via the formation of hydroxyl and sulfate radicals, Water Res., 47 (2013) 5431–5438.
[26] R. Yuan, S.N. Ramjaun, Z. Wang, J. Liu, Effects of chloride ion on degradation of Acid orange 7 by sulfate radical-based advanced oxidation process: implications for formation of chlorinated aromatic compounds, J. Hazard. Mater., 196 (2011) 173–179.
[27] P. Nfodzo, H. Choi, Triclosan decomposition by sulfate radicals: effects of oxidant and metal doses, Chem. Eng. J., 174 (2011) 629–634.
[28] A. Rastogi, S.R. Al-Abed, D.D. Dionysiou, Sulfate radical-based ferrous-peroxymonosulfate oxidative system for PCBs degradation in aqueous and sediment systems, Appl. Catal., B, 85 (2009) 171–179.
[29] J.G. Huang, J.J. Chen, Z.M. Xie, X.J. Xu, Treatment of nanofiltration concentrates of mature landfill leachate by a coupled process of coagulation and internal micro-electrolysis adding hydrogen peroxide, Environ. Technol., 36 (2015) 1001–1007.
[30] R.L. Johnson, P.G. Tratnyek, R.O.B. Johnson, Persulfate persistence under thermal activation conditions, Environ. Sci. Technol., 42 (2008) 9350–9356.
[31] V.C. Mora, J.A. Rosso, G. Carrillo Le Roux, D.O. Mártire, M.C. Gonzalez, Thermally activated peroxydisulfate in the presence of additives: a clean method for the degradation of pollutants, Chemosphere, 75 (2009) 1405–1409.
[32] C. Liang, C.J. Bruell, Thermally activated persulfate oxidation of trichloroethylene: experimental investigation of reaction orders, Ind. Eng. Chem. Res., 47 (2008) 2912–2918.
[33] H. Zhang, Z. Wang, C.C. Liu, Y.Z. Guo, N. Shan, C.X. Meng, L.Y. Sun, Removal of COD from landfill leachate by an electro/Fe^{2+}/peroxydisulfate process, Chem. Eng. J., 250 (2014) 76–82.
[34] G.P. Anipsitakis, D.D. Dionysiou, M.A. Gonzalez, Cobalt-mediated activation of peroxymonosulfate and sulfate radical attack on phenolic compounds. Implications of chloride ions, Environ. Sci. Technol., 40 (2006) 1000–1007.
[35] J. De Laat, T.G. Le, Kinetics and modeling of the Fe(III)/H_2O_2 system in the presence of sulfate in acidic aqueous solutions, Environ. Sci. Technol., 39 (2005) 1811–1818.
[36] M.J.K. Bashir, H.A. Aziz, S.Q. Aziz, S.A. Amr, An Overview of Wastewater Treatment Processes Optimization Using Response Surface Methodology (RSM), The 4th International Engineering Conference – Towards Engineering of 21st Century, Filistin, 1–11, 15–16 of October 2012.
[37] E. Gengec, M. Kobya, E. Demirbas, A. Akyol, K. Oktor, Optimization of baker's yeast wastewater using response surface methodology by electrocoagulation, Desalination, 286 (2012) 200–209.
[38] APHA, Standard Methods for the Examination of Water and Wastewater, American Public Health Association, Washington, D.C., USA, 2005.
[39] M. Ahmadi, F. Vahabzadeh, B. Bonakdarpour, E. Mofarrah, M. Mehranian, Application of the central composite design and response surface methodology to the advanced treatment of olive oil processing wastewater using Fenton's peroxidation, J. Hazard. Mater., 123 (2005) 187–195.
[40] J.P. Wang, Y.Z. Chen, X.W. Ge, H.Q. Yu, Optimization of coagulation–flocculation process for a paper-recycling wastewater treatment using response surface methodology, Colloids Surf., A, 302 (2007) 204–210.
[41] T. Ölmez, The optimization of Cr(VI) reduction and removal by electrocoagulation using response surface methodology, J. Hazard. Mater., 162 (2009) 1371–1378.
[42] R.H. Myers, Response surface methodology – current status and future directions, J. Qual. Technol., 31 (1999) 30–44.
[43] X.B. Zhu, J.P. Tian, R. Liu, L.J. Chen, Optimization of Fenton and electro-Fenton oxidation of biologically treated coking wastewater using response surface methodology, Sep. Purif. Technol., 81 (2011) 444–450.
[44] I. Arslan-Alaton, G. Tureli, T. Olmez-Hanci, Treatment of azo dye production wastewaters using photo-Fenton-like advanced oxidation processes: optimization by response surface methodology, J. Photochem. Photobiol., A, 202 (2009) 142–153.
[45] M. Umar, H.A. Aziz, M.S. Yusoff, Assessing the chlorine disinfection of landfill leachate and optimization by response surface methodology (RSM), Desalination, 274 (2011) 278–283.
[46] S. Bajpai, S.K. Gupta, A. Dey, M.K. Jha, V. Bajpai, S. Joshi, A. Gupta, Application of central composite design approach for removal of chromium(VI) from aqueous solution using weakly anionic resin: modeling, optimization, and study of interactive variables, J. Hazard. Mater., 227–228 (2012) 436–444.
[47] X.B. Jing, Y. Cao, X. Zhang, D.H. Wang, X.Z. Wu, H. Xu, Biosorption of Cr(VI) from simulated wastewater using a cationic surfactant modified spent mushroom, Desalination, 269 (2011) 120–127.
[48] K. Ravikumar, S. Krishnan, S. Ramalingam, K. Balu, Optimization of process variables by the application of response surface methodology for dye removal using a novel adsorbent, Dyes Pigm., 72 (2007) 66–74.
[49] A.A. Ahmad, B.H. Hameed, A.L. Ahmad, Removal of disperse dye from aqueous solution using waste-derived activated carbon: optimization study, J. Hazard. Mater., 170 (2009) 612–619.
[50] A.A.L. Zinatizadeh, A.R. Mohamed, A.Z. Abdullah, M.D. Mashitah, M. Hasnain Isa, G.D. Najafpour, Process modeling and analysis of palm oil mill effluent treatment in an up-flow anaerobic sludge fixed film bioreactor using response surface methodology (RSM), Water Res., 40 (2006) 3193–3208.
[51] H.S. Li, S.Q. Zhou, Y.B. Sun, J. Lv, Application of response surface methodology to the advanced treatment of biologically stabilized landfill leachate using Fenton's reagent, Waste Manage., 30 (2010) 2122–2129.
[52] Q.K. Beg, V. Sahai, R. Gupta, Statistical media optimization and alkaline protease production from *Bacillus mojavensis* in a bioreactor, Process Biochem., 39 (2003) 203–209.
[53] J. Kumar, A. Bansal, Photocatalytic degradation in annular reactor: modelization and optimization using computational fluid dynamics (CFD) and response surface methodology (RSM), J. Environ. Chem. Eng., 1 (2013) 398–405.
[54] N. Rastkari, A. Eslami, S. Nasseri, E. Piroti, A. Asadi, Optimizing parameters on nanophotocatalytic degradation of ibuprofen using UVC/ZnO processes by response surface methodology, Pol. J. Environ. Stud., 26 (2017) 785–794.
[55] M. Ahmadi, F. Ghanbari, S. Madihi-Bidgoli, Photoperoxi-coagulation using activated carbon fiber cathode as an efficient method for benzotriazole removal from aqueous solutions: modeling, optimization and mechanism, J. Photochem. Photobiol., A, 322–323 (2016) 85–94.
[56] M. Ahmadi, F. Ghanbari, M. Moradi, Photocatalysis assisted by peroxymonosulfate and persulfate for benzotriazole degradation: effect of ph on sulfate and hydroxyl radicals, Water Sci. Technol., 72 (2015) 2095–2102.
[57] R. Hazime, Q.H. Nguyen, C. Ferronato, A. Salvador, F. Jaber, J.M. Chovelon, Comparative study of imazalil degradation in three systems: UV/TiO_2, UV/$K_2S_2O_8$ and UV/TiO_2/$K_2S_2O_8$, Appl. Catal., B, 144 (2014) 286–291.
[58] S. Akbari, F. Ghanbari, M. Moradi, Bisphenol A degradation in aqueous solutions by electrogenerated ferrous ion activated ozone, hydrogen peroxide and persulfate: applying low current density for oxidation mechanism, Chem. Eng. J., 294 (2016) 298–307.
[59] Y.F. Rao, L. Qu, H.S. Yang, W. Chu, Degradation of carbamazepine by Fe(II)-activated persulfate process, J. Hazard. Mater., 268 (2014) 23–32.
[60] N. Jaafarzadeh, M. Omidinasab, F. Ghanbari, Combined electrocoagulation and UV-based sulfate radical oxidation processes for treatment of pulp and paper wastewater, Process Saf. Environ. Prot., 102 (2016) 462–472.
[61] X. Zhou, Z.L. Hou, L. Lv, J.J. Song, Z.Y. Yin, Electro-Fenton with peroxi-coagulation as a feasible pre-treatment for high-strength

refractory coke plant wastewater: parameters optimization, removal behavior and kinetics analysis, Chemosphere, 238 (2020) 124649.
[62] E. Pajootan, M. Arami, M. Rahimdokht, Application of carbon nanotubes coated electrodes and immobilized TiO_2 for dye degradation in a continuous photocatalytic-electro-Fenton process, Ind. Eng. Chem. Res., 53 (2014) 16261–16269.
[63] P.V. Nidheesh, R. Gandhimathi, Trends in electro-Fenton process for water and wastewater treatment: an overview, Desalination, 299 (2012) 1–15.
[64] S. Ahmadzadeh, M. Dolatabadi, Modeling and kinetics study of electrochemical peroxidation process for mineralization of bisphenol A; a new paradigm for groundwater treatment, J. Mol. Liq., 254 (2018) 76–82.
[65] E.S.Z. El-Ashtoukhy, N.K. Amin, O. Abdelwahab, Treatment of paper mill effluents in a batch-stirred electrochemical tank reactor, Chem. Eng. J., 146 (2009) 205–210.
[66] W.M. Chen, Z.P. Gu, P. Wen, Q.B. Li, Degradation of refractory organic contaminants in membrane concentrates from landfill leachate by a combined coagulation-ozonation process, Chemosphere, 217 (2019) 411–422.
[67] A.P. Zhang, Z.P. Gu, W.M. Chen, Q.B. Li, G.B. Jiang, Removal of refractory organic pollutants in reverse-osmosis concentrated leachate by microwave–Fenton process, Environ. Sci. Pollut. Res., 25 (2018) 28907–28916.
[68] H. Wang, Y.H. Wang, Z.Y. Lou, N.W. Zhu, H.P. Yuan, The degradation processes of refractory substances in nano-filtration concentrated leachate using micro-ozonation, Waste Manage., 69 (2017) 274–280.
[69] R. Sridhar, V. Sivakumar, V. Prince Immanuel, J. Prakash Maran, Treatment of pulp and paper industry bleaching effluent by electrocoagulant process, J. Hazard. Mater., 186 (2011) 1495–1502.